This is a repository copy of *Preventing and repairing myeloma bone disease by combining conventional antiresorptive treatment with a bone anabolic agent in murine models*.

Version: Accepted Version

Original Article

Title: Preventing and repairing myeloma bone disease by combining conventional antiresorptive treatment with a bone anabolic agent in murine models[†]

Authors: *Julia Paton-Hough, PhD[1,2] (j.paton-hough@sheffield.ac.uk), *Simon Tazzyman, PhD[1,2] (s.tazzyman@sheffield.ac.uk), Holly Evans, BSc[1,2] (h.r.evans@sheffield.ac.uk), Darren Lath, MPhil[1,2] (d.lath@sheffield.ac.uk), Jenny M. Down[1,2] (j.m.down@sheffield.ac.uk), Alanna. C. Green, PhD[1,2] (a.c.green@sheffield.ac.uk), John A. Snowden[3] (john.snowden@sth.nhs.uk), MD, **Andrew D. Chantry, PhD, MD[1,2,3] (a.d.chantry@sheffield.ac.uk) & **Michelle A. Lawson, PhD[1,2] (m.a.lawson@sheffield.ac.uk).

*Joint first authors **Joint senior authors

Affiliations:

[1]Sheffield Myeloma Research Team, Department of Oncology and Metabolism, Medical School, University of Sheffield, Beech Hill Road, Sheffield, S10 2RX, UK.

[2]Mellanby Centre for Bone Research, University of Sheffield Medical School, University of Sheffield, Beech Hill Road, Sheffield, S10 2RX, UK.

[3]Department of Haematology, Sheffield Teaching Hospitals NHS Foundation Trust, Royal Hallamshire Hospital, Glossop Road, Sheffield, S10 2JF, UK.

Corresponding author:
Dr Michelle Lawson
The University of Sheffield Medical School
Beech Hill Road, Sheffield
S10 2RX
m.a.lawson@sheffield.ac.uk
+44 (0)114 2159054

Abstract

Multiple myeloma is a plasma cell malignancy, which develops in the bone marrow and frequently leads to severe bone destruction. Current antiresorptive therapies to treat the bone disease do little to repair damaged bone; therefore, new treatment strategies incorporating bone anabolic therapies are urgently required. We hypothesized that combination therapy using the standard of care antiresorptive zoledronic acid (Zol) with a bone anabolic (anti-TGFβ/1D11) would be more effective at treating myeloma-induced bone disease than Zol therapy alone. JJN3 myeloma-bearing mice (n=8/group) treated with combined Zol and 1D11 resulted in a 48% increase (p≤0.001) in BV/TV compared to Zol alone and a 65% increase (p≤0.0001) compared to 1D11 alone. Our most significant finding was the substantial repair of U266-induced osteolytic bone lesions with combination therapy (n=8/group), which resulted in a significant reduction in lesion area compared to vehicle (p≤0.01) or Zol alone (p≤0.01). These results demonstrate that combined antiresorptive and bone anabolic therapy is significantly more effective at preventing myeloma-induced bone disease than Zol alone. Furthermore, we demonstrate that combined therapy is able to repair established myelomatous bone lesions. This is a highly translational strategy which could significantly improve bone outcomes and quality of life for patients with myeloma. This article is protected by copyright. All rights reserved

Introduction

Multiple myeloma is a cancer of plasma cells which frequently causes severe bone destruction and debilitating bone pain, resulting in substantially diminished functional capacity and quality of life (1, 2). Across a retrospective study, approximately 80% of all myeloma patients experienced pathological fractures and 90% had osteolytic bone lesions over the course of disease (3), which correlates with poor survival and mortality (4). Myeloma-induced bone disease occurs via several mechanisms. In most cases, osteoclast stimulating factors including receptor activator of nuclear factor kappa (κ) β ligand (RANKL) (5, 6), macrophage inflammatory protein 1 (7, 8) and various interleukins (IL-1β (9), IL-3 (10), IL-6 (11)) are produced by myeloma cells or tumor-activated cells in the bone marrow microenvironment (BMME), causing an increase in bone resorption. In addition, osteoblast inhibitors such as dickkopf-1 (Dkk-1) (12, 13), activin A (14, 15) and sclerostin (16, 17) are upregulated in patient sera resulting in a decrease in bone formation. Overall, this imbalance of bone remodelling results in severe bone loss. Myeloma patients presenting with bone disease are commonly prescribed the antiresorptive agent zoledronic acid (Zol) (18). However, whilst Zol and other antiresorptives are effective at inhibiting osteoclastic bone resorption they do virtually nothing to repair existing bone damage, and as a result bone remains weak and at risk of fracture.

Bone anabolic therapies using inhibitors of activin A (15) and Dkk-1 (19, 20) have shown promise in preclinical models of myeloma but thus far have resulted in only modest benefit in clinical trials (21-23), and have also led to some unexpected side effects. For example, rises in haematocrit after treatment with Sotatercept, a decoy receptor for activin A, have been observed, leading to a re-purposing of this and similar agents as a treatment for cancer-induced anaemia (21). More recently, deletion of the sclerostin gene (Sost) or administration of an anti-

sclerostin antibody prevented bone disease in murine models of myeloma (24). Furthermore, when an anti-sclerostin treatment was used in combination with Zol in preclinical models of myeloma, using a preventative regimen, they showed superior effects on fracture resistance compared to Zol alone (25). However, sclerostin's effectiveness on established osteolytic bone disease has not yet been assessed in murine models or in patients with myeloma. In osteoporotic patients, anti-sclerostin therapy (Romosozumab) was associated with a lower risk of fracture (26), but was also associated with potential adverse cardiac events (27). In addition, the positive effects of anti-sclerostin therapy upon bone formation were only sustained for a short period (26). Furthermore, a combination of Dkk-1 and sclerostin inhibition using a bi-specific antibody approach demonstrated great promise at increasing bone formation and bone strength in naïve rodents, and therefore would be a desirable method to test in preclinical models of myeloma (28).

As indicated, there is a clear demand for new bone anabolic agents for patients with myeloma and established osteolytic bone disease. It is hoped that such therapies will enhance bone formation for sustained periods, leading to repair of damaged bones. This has clear translational potential for substantially improving the morbidity and quality of life in terms of fracture risk, pain control and functional status for patients with myeloma bone disease.

A potential therapeutic target in myeloma is TGFβ, which is a cytokine reported to have both inhibitory (29, 30) and stimulatory (31, 32) roles in bone formation. Specifically, it is known to inhibit osteoblast differentiation. TGFβ is also known to be expressed by patient myeloma cells (33, 34), is upregulated in sera from some monoclonal gammopathy of undetermined significance (MGUS) patients (35) and is associated with immunoparesis in myeloma patients at various stages of the disease (36). It has also been shown to be over expressed by bone

marrow stromal cells (BMSC) from myeloma patients (34) and is liberated from bone mineral matrix undergoing resorption. TGFβ's actions can be blocked using a TGFβRI inhibitor (SD-208) in vitro (37) and, more recently, TGFβ inhibition has been used as anti-tumor therapy in preclinical models of myeloma (38, 39), breast cancer (40-42) and prostate cancer (43). Interestingly, several of these inhibitors are now in cancer clinical trials as anti-tumor drugs (e.g. NCT02452008 and NCT01401062 (44, 45)). However, TGFβ inhibition has been shown to have direct bone anabolic effects in naïve animals, resulting in increased bone formation and bone integrity (29). This complements findings from immune competent models of myeloma where TGFβ inhibition results in significantly higher vertebral strength and fewer femoral osteolytic lesions compared to control mice (46). Currently, no studies have explored the efficacy of bone anabolic therapy in combination with an antiresorptive specifically to evaluate whether repair of existing osteolytic lesions is possible (previous studies have only focussed on preventing the development of bone lesions at the end stage of disease). Here we show that bone anabolic therapy using an anti-TGFβ (1D11) antibody combined with the standard of care antiresorptive Zol are able to repair existing osteolytic lesions, and are more effective at repairing osteolytic lesions and preventing myeloma bone disease, than either therapy alone.

Materials & Methods

Ethics statement

All procedures involving animals were conducted at the University of Sheffield (UK) and were approved by the Home Office (PPL 70/8799) and the University of Sheffield's Animal Ethics Committee in accordance with the Animal [Scientific Procedures] Act 1986.

Osteoblast isolation and differentiation

Primary calvarial osteoblast-like cells (Ob-LC) were isolated and differentiated as described previously (47) using 4% FCS and BMP-2 (30 ng/ml) (Bio-Techné, Abingdon, UK). To determine the effect of TGFβ upon osteoblast differentiation, Ob-LC were cultured with either vehicle (CTRL), recombinant TGFβ1 (rTGFβ1) (5 ng/ml) and mouse IgG1 isotype control (IC) antibody (25 µg/ml) (Bio-Techné) (rTGFβ + IC) or rTGFβ1 (5 ng/ml) and 1D11 antibody (25 µg/ml) (Bio-Techné), (rTGFβ + 1D11). Media was changed every 2-3 days and differentiation was assessed at 7 and 14 days after treatment began by examining alkaline phosphatase (Alp), and at 14 and 21 days using alizarin red staining to detect mineralization, described previously (48). Osteosarcoma SAOS-2 cells (ATCC, Teddington, UK) cultured as described previously (49), were treated as above for 3 days and cultured in 1% FCS to measure Alp. Each experiment was repeated at least three times (n=3) and representative data are presented as a fold change.

Osteoclast assays

Bone marrow osteoclasts were isolated and cultured from 4 week old female BALB/c mice as previously described (50). Cells were then treated with either vehicle (CTRL), IC (25 µg/ml) or 1D11 (25 µg/ml) every 2-3 days for 14 days. Osteoclast numbers and resorption area were then analyzed as previously described (50).

Myeloma cell viability assays

JJN3 and U266 human myeloma cell lines were cultured in RPMI-1640 medium (containing 10% FCS, 1% penicillin/streptomycin, 100 U/100 μg/ml, 1% non-essential amino acids and 1% sodium pyruvate, 1 mM) at 37°C in 5% CO_2. Cells were seeded (at 2×10^4 cells/well) in triplicate in 96 well plates and treated with either vehicle (CTRL), IC (25 µg/ml) or 1D11 (25

µg/ml). After 4 h, 24 h, 48 h and 72 h, cell viability was measured using an Alamar®Blue assay (Thermofisher, Warrington, UK) according to the manufacturer's instructions.

ELISA

ELISA was used to detect murine TRAP5b (Oxford Biosystems, Oxford, UK), murine P1NP (Immuno Diagnostic Systems, Tyne & Wear, UK), murine IL-6 (Abcam, Cambridge, UK) and human IgE paraprotein (Thermofisher) in murine sera following the manufacturer's instructions.

In vivo studies

Nod/Scid γ (NSG, NOD.Cg-Prkdcscid Il2rgtm1Wjl/SzJ) mice were purchased from Charles River Laboratories (UK). Animal numbers were calculated using G*Power software recommended by NC3Rs. All animals were housed in the Biological Service Unit at the University of Sheffield in individual ventilated cages. Both an aggressive myeloma model using JJN3 cells and a moderately aggressive model using U266 cells were used in the in vivo experiments. In NSG mice these cell types specifically colonise the bone following intravenous (i.v) injection with no extramedullary growth resulting in bone disease as described previously (51-53).

The effect of 1D11 in naïve and JJN3-bearing NSG mice

7-8 week old female NSG mice were randomised into groups (n=5/group) and injected i.v via the tail vein with 100 µl PBS (Naïve) or $1x10^6$ JJN3 cells (JJN3). After 7 days, mice were treated with either 20 mg/kg IgG1 IC (Naïve + IC/ JJN3 + IC) or 20 mg/kg 1D11 (Naïve + 1D11/ JJN3 + 1D11) via intraperitoneal (i.p) injection every three days and mice were culled after 21 days post tumor cell injection.

Mouse group numbers were ascertained through the use of the power calculation formula:

$$2(SD)^2 \; x \; f(\alpha,\beta)/\Delta^2$$

where α (significance level) was 0.05, β (power level) was 90%, and both Δ (least practicable difference between groups) and standard deviation were taken from a similar study with regard to percentage trabecular bone volume (BV/TV, bone volume/total volume). It gave rise to the following power calculation:

$$2(1.4)^2 \; x \; 10.5/3^2 = 4.6, \text{ i.e. 5 mice.}$$

Assessment of tumor burden and bone disease (ex vivo)

At the end of the experiment mice were euthanized and the bone marrow from the left femora were flushed and tumor burden was assessed by anti-human leukocyte antigen (HLA) staining analyzed by flow cytometry using a FACS Calibur and Cell quest software (BD Biosciences Illinois, USA) as described previously (54). Tumor burden was also quantified in haematoxylin stained paraffin embedded sections, which were scanned using a Hamamatsu Nanozoomer XR (Hamamatsu City, Japan) and analyzed by morphology as a percentage of the bone marrow using Image Scope software (Leica Biosystems, Illinois, USA). To assess bone disease, following mouse euthanasia, the right and left tibiae were analyzed by μCT using a SkyScan 1272 ex vivo μCT scanner at 50 kilovolts (kV) and 200 microamperes (μA), using an aluminium filter of 0.5 mm and pixel size of 4.3 μm^2 as described previously (19, 51). BV/TV, trabecular number, trabecular thickness, cortical thickness, lesion area and lesion number parameters were then assessed as described previously (51) and according to standard guidelines (55). 3-D models of trabecular bone were created using ParaView Software (New York, USA). Histomorphometry was used to detect differences in osteoblast and osteoclast numbers on longitudinal bone sections using Osteomeasure software (Georgia, USA), as

described previously (51) and following standard guidelines (56).

Efficacy of 1D11 and Zol combination therapy in the JJN3 murine model of MM

8-9 week old female mice were randomised into groups (n=8/group) and treated as follows: Group 1, PBS i.v (Naïve); Group 2, 1×10^6 JJN3 cells i.v and IC (20 mg/kg IgG1, i.p every 3 days post tumor cell injection) (JJN3); Group 3, JJN3 cells and Zol (Proctor & Gamble, 125 µg/kg subcutaneously (s.c) on days 13 and 16 post tumor cell injection) and IC (Zol); Group 4, JJN3 cells and 1D11 (20 mg/kg, i.p every 3 days post tumor cell injection) (1D11) or; Group 5, JJN3 cells, Zol and 1D11 (Combo). After 21 days post tumor cell injection all animals were sacrificed. Tumor burden and bone disease were assessed as described above. Murine P1NP, TRAP5b and IL-6 serum levels were quantified by ELISA as described above.

Mouse group numbers were determined using the same power calculation formula shown above. α was taken as 0.05, β was taken as 90%, and Δ and SD values were taken from the results of the 'effect of 1D11 in naïve and JJN3-bearing NSG mice' study described above with regard to percentage BV/TV. It gave rise to the following power calculation:

$$2(1.8)^2 \times 10.5/3^2 = 7.6, \text{ i.e. 8 mice}$$

Longitudinal monitoring of lesion repair following 1D11 and Zol combination therapy in the U266 murine model of myeloma

22 female NSG mice (7-8 weeks old) were injected i.v with 1×10^6 U266 cells. At 5 weeks post-tumor cell injection, bone disease progression was monitored twice a week in the right tibiae of each mouse using a VivaCT 80 in vivo preclinical µCT scanner (Scanco, Zurich, Switzerland) as described below. Upon detection of established osteolytic lesions (at approximately 6 weeks post U266 injection), mice were randomly split into three groups and

treated as follows: Group 1, vehicle (U266); Group 2, Zol (125 μg/kg s.c, 3 days apart) and IC (20 mg/kg IgG1, i.p, every 3 days) (Zol) or; Group 3, 1D11 (20 mg/kg, i.p every 3 days) and Zol (Combo). Mice were culled 3 weeks post-treatment (Group 1, n=6; Group 2, n=8; and Group 3, n=8) and tumor burden was assessed by flow cytometry (HLA staining), histology (morphology) and ELISA (IgE paraprotein levels) as described above.

Mouse group numbers were determined using the same power calculation shown above:

$$2(1.8)^2 \text{ x } 10.5/3^2 = 7.6, \text{ i.e. 8 mice.}$$

However, due to a smaller cohort than anticipated only 6 mice were available for the vehicle group. This was deemed acceptable as the vehicle group was less variable than the treatment groups with regards to bone lesion development, based on previously published data (51).

Bone disease assessment (in vivo)

Mice were anaesthetized and right tibiae were scanned using a VivaCT 80 at 45 kV and 177 μA with a voxel size of 10.4 μm on Week 0 (W0; when bone disease was first detected following tumor cell inoculation, at approximately 6 weeks) and then again after 3 weeks (W3). For image registration, W3 tibia datasets were registered to their paired W0 control datasets using MIM Maestro (v. 6.6.6, Ohio, USA). Following registration, both datasets were volumetrically registered using Drishti software (v. 10, ANU Vizlab, Australia) and quantified using ImageJ (version 1.47, NIH, USA). The percentage change in lesion area, cortical thickness and BV/TV was then calculated from time of disease onset (W0) to three weeks post treatment (W3), presented as the mean percentage change for each group. 3-D transverse models of the tibiae were created using ParaView software (New York, USA) and 3-D longitudinal models of the tibiae were created using Drishti software (Acton, Australia).

Statistical analysis

All data were analyzed using GraphPad Instat version 6.0b (California, USA). Where possible, the distribution of data was analyzed using a D'Agostino-Pearson omnibus normalisation test and relevant parametric or non-parametric statistical tests were used. If normalization was not possible, normal distribution was assumed and data was analyzed using either a Student's T-Test or one-way ANOVA with a Tukey's multiple comparison test. Where data was not normally distributed, a non-parametric Kruskal-Wallis test followed by a Dunn's multiple comparison test was used. Any potential outliers were identified using Grubb's outlier analysis and removed accordingly. All data were expressed with error bars representing mean ± standard deviation (SD).

Data sharing

Data will be accessible to the public following publication via ORDA, the University of Sheffield's Research Data Catalogue and Repository. All data is preserved for 10 years and those interested in obtaining access to this data must contact the first author via email.

Results

TGFβ inhibition restores osteoblast differentiation in vitro and has a bone anabolic effect in vivo

TGFβ, as described above, is secreted by patient myeloma cells and BMSC (34) and is also liberated from bone matrix upon resorption (57). Importantly, TGFβ is also an inhibitor of osteoblast differentiation, thus contributing to the mechanism of bone disease in myeloma patients. Therefore, we wanted to firstly confirm that blocking TGFβ using a monoclonal anti-

TGFβ antibody (1D11) would prevent rTGFβ1 inhibition of osteoblast differentiation, and secondly that 1D11 would result in a bone anabolic effect in naïve and tumor-bearing mice.

Treatment of primary murine calvarial Ob-LC with rTGFβ1 resulted in a 52% ($p \leq 0.001$) and 58% ($p \leq 0.01$) reduction in Alp at 7 and 14 days, respectively, which was prevented upon treatment with 1D11 at both time points ($p \leq 0.01$) (Figure 1a i-ii). This effect was also observed using the human osteosarcoma cell line SAOS-2 (Figure 1a iii). In addition, rTGFβ1 inhibited Ob-LC mineralisation by 89% at 14 days ($p \leq 0.01$) and 88% at 21 days ($p \leq 0.001$), this was also prevented following treatment with 1D11 ($p \leq 0.01$, $P \leq 0.001$, respectively) (Figure 1a iv-vi). This confirmed similar results reporting that TGFβ prevents osteoblast differentiation in MC3T3-E1, C2C12 cells and primary BMSC from myeloma patients, an effect which could be blocked by TGFβ inhibition (39, 58).

We then verified the translational efficacy of this concept in vivo by administering 1D11 into naïve mice and mice bearing JJN3 myeloma cells (treatment schedule described in Figure 1b). 1D11 treatment in vivo resulted in a significant increase in BV/TV in both naïve (130%) ($p \leq 0.01$) and JJN3-bearing mice (183%) ($p \leq 0.001$) compared to IC treated animals (Figure 1c i-v). JJN3-bearing mice treated with 1D11 also had a higher trabecular number (Figure 1c vi) ($p \leq 0.01$), whereas naïve, but not JJN3-bearing, mice treated with 1D11 had thicker trabeculae (Figure 1c vii) ($p \leq 0.01$). These data confirmed previous reports that 1D11 was a bone anabolic agent in naïve mice (29) and prevented trabecular bone loss in immune competent myeloma-bearing animals (46).

TGFβ inhibition (1D11) in combination with Zol significantly increased trabecular bone volume compared to monotherapy with either agent in the JJN3 model of myeloma

Since 1D11 promoted bone formation in naïve mice (Figure 1c i-ii) and prevented bone loss in JJN3-bearing mice (Figure 1c iii-iv), we investigated whether administration with the antiresorptive Zol, would further enhance the bone anabolic effect of 1D11 in the JJN3 model of myeloma (treatment schedule described in Figure 2a). Zol alone significantly increased BV/TV (p≤0.01) compared to tumor control (Figure 2b i-ii, v) (confirming previous findings (51)). Similarly, 1D11 prevented bone loss compared to the tumor control group (Figure 2b i, iii, v), confirming our previous data (Figure 1c iii-v). Most interestingly, when Zol and 1D11 were given in combination, BV/TV was 48% higher (p≤0.001) compared to Zol (Figure 2b ii, iv, v) and 65% higher (p≤0.0001) compared to 1D11 alone (Figure 2b iii, iv, v). The trabecular number was also significantly higher in the combination group compared to Zol alone (Figure 2b vi) (p≤0.001), whereas there were no significant changes in thickness of the trabeculae between the Zol, 1D11 or the combination groups (Figure 2b vii). In contrast to trabecular bone, cortical bone thickness was comparable between naïve and JJN3-bearing mice (Figure 2c v), indicating JJN3 tumor cells did not cause significant loss of cortical bone. Zol and 1D11 monotherapies had no effect on cortical thickness compared to vehicle controls. However, cortical thickness was higher in mice receiving combination therapy compared to 1D11 alone (Figure 2c iii, iv, v). Analysis of osteolytic lesions in the cortical bone revealed vehicle-treated JJN3-bearing mice had an average of 26±13.8 lesions in the area analyzed (Figure 2c vi), and 1D11 monotherapy had no effect on lesion number or size compared to the JJN3 with vehicle (Figure 2c vi, vii). In comparison, administration of Zol over 2 weeks was highly effective at preventing osteolytic lesion development in mice, with only 4±1.9 lesions present (Figure 2c vi). Similarly, mice treated with Zol and 1D11 in combination had virtually no cortical bone lesions, with only 2±2.5 lesions per mouse in the area analyzed (Figure 2c vi). Whilst osteolytic

lesion number and size were slightly lower in mice treated with the combination compared to Zol treatment alone, this was not significant as Zol treatment alone prevented the development of virtually all lesions in mice.

Overall, this study clearly shows that TGFβ inhibition therapy when combined with Zol was more effective at preventing trabecular bone loss than either monotherapy alone in an aggressive murine model of myeloma.

To determine whether these observations were mediated via a bone anabolic or antiresorptive effect, histological analysis was conducted by quantifying osteoblast and osteoclast numbers on endocortical and trabecular bone surfaces in the primary spongiosa. Unexpectedly, when osteoblast numbers were analyzed there were no significant differences between any of the tumor groups looking at the end stage of disease (Figure 3a i-x). However, 1D11 treatment did result in fewer osteoclasts on endocortical bone surfaces (42%) (p≤0.05) and in the primary spongiosa region (47%) (p≤0.0001) (Figure 3a i, iii, v, vii, xi, xii), which was more pronounced with Zol treatment and resulted in even fewer osteoclasts on the endocortical surface (85%) (p≤0.0001) and primary spongiosa (88%) (p≤0.0001) compared to JJN3 IC treated animals (Figure 3a i, ii, v, vi, xi, xii). In mice receiving combination treatment, trabecular and endocortical osteoclast numbers were comparable to monotherapy of Zol with no further reduction in osteoclast numbers (Figure 3a ii, iv, vi, viii, xi, xii), though as Zol alone reduced osteoclast numbers to effectively zero it is impossible to ascertain whether there would have been a further reduction with the combination treatment. To further investigate the effect of combination therapy on bone resorption and formation, systemic analysis of bone turnover markers TRAP5b and P1NP in mouse sera was also conducted at the end stage of disease. TRAP5b concentrations in Zol treated animals correlated with the histological osteoclast data,

whereby Zol alone significantly reduced TRAP5b levels compared to tumor (p≤0.05), but this was not observed in the 1D11 alone group (Figure 3b i). Therefore, we assessed the effects of 1D11 on primary murine osteoclasts in vitro and observed a significant reduction in their numbers (Figure 3b ii) and resorption area (Figure 3b iii) compared to controls (vehicle and IC). However despite this, TRAP5b serum levels in the in vivo study were not further reduced in the combination treatment group compared to Zol alone, which was consistent with the histological osteoclast data. P1NP levels also correlated with the histological osteoblast data, where at the end stage of disease circulating levels were unchanged between all groups (Figure 3b iv),

We sought to understand why osteoclast numbers were decreased by ID11 treatment and chose to investigate the role of IL-6. Previously, IL-6 has been shown to be upregulated in myeloma patient sera (59) and by BMSC, particularly when in contact with myeloma cells (57), and IL-6 is thought to increase the proliferation/differentiation of osteoclasts (60). TGFβ is also known to upregulate the production of IL-6 by BMSC, the effect of which can be blocked using a TGFβ signalling antagonist (SD-208, a small molecule inhibitor) (37). Therefore, TGFβ in myeloma is also likely to contribute to bone disease by upregulation of IL-6 in the BMME. Consequently, we investigated IL-6 in the sera of mice at the end stage of disease and found that IL-6 levels were unchanged in tumor control or Zol treated mice, but were significantly reduced in mice treated with either 1D11 alone or 1D11 in combination with Zol (p≤0.05 and p≤0.001, respectively) (Figure 3b v). It is therefore suggested that this IL-6 reduction was specific to the 1D11 treatment with no additive or synergistic effect with Zol.

Overall, using the JJN3 model of MM, combination therapy showed a clear additive effect upon increasing trabecular bone. However, limitations of this 3-week model of myeloma, i.e.

the rapidly progressive osteolytic phenotype, made it difficult to identify if combination therapy was more effective than monotherapy at protecting against or repairing myeloma bone disease in the cortical bone. We therefore chose to investigate the effects of combination therapy in the U266 model of myeloma, which also features a marked destructive bone phenotype, but develops less quickly over a more protracted period (after 6-9 weeks post tumor cell injection).

Established U266-induced osteolytic lesions are repaired with combined TGFβ inhibition (1D11) and Zol therapy

To determine whether anti-TGFβ therapy was capable of repairing existing osteolytic bone lesions in tumor-bearing mice, we monitored changes to bone over time in the same mice using in vivo μCT. The U266 murine model of myeloma is less aggressive than the JJN3 model used above, whereby osteolytic bone lesions in U266-bearing mice typically evolve more slowly and can take up to 5-6 weeks to develop (treatment schedule described in Figure 4a). Bone disease on 3-D transverse (Figure 4b) and longitudinal (Figure 4c) μCT models was apparent from 6 weeks post-tumor cell injection (W0) (Figure 4b i, iii, v, Figure 4c i, iii, v, blue arrows) and became progressively worse over the subsequent 3 weeks (W3) (Figure 4b ii, Figure 4c ii, pink arrows). U266-bearing mice treated with Zol alone, however, had areas of both progressive lesion development (Figure 4b iii, iv, Figure 4c iii, iv, pink arrows) and lesion repair by W3 (Figure 4b iii-iv, green arrows). Most strikingly, the Zol and 1D11 combination group did not show progressive bone disease, and the initial regions of bone loss were substantially repaired by week 3 (Figure 4b v, vi, Figure 4c v, vi, green arrows). When quantified, there was a significant decrease in lesion area in the combination group compared to the Zol alone (Figure 4c vii) (p≤0.05) and vehicle (p≤0.05) groups. However, when overall cortical thickness and BV/TV were analyzed in this model, these parameters were not

significantly different between the Zol alone and combination group but were significantly increased compared to the U266 vehicle group (p≤0.05, Figure 4b viii, ix).

To explore the mechanism of this repair we conducted histomorphometric and serum bone turnover marker analysis. Similar to the data acquired in the JJN3 combination study (Figure 3), U266-bearing mice treated with Zol alone or with the combination group effectively reduced the numbers of osteoclasts by 64% (p≤0.0001) and 66% (p≤0.0001) respectively on the endocortical surface compared to the U266 vehicle group (Figure 5 i-vii). In addition, osteoclasts were significantly reduced in the primary spongiosa by 54% (p≤0.05) in the Zol group and 51% (p≤0.05) in the combination group compared to U266 vehicle group (Figure 5 viii). TRAP5b levels also correlated with histomorphometric analysis, whereby Zol alone and in combination with 1D11 reduced TRAP5b compared to the U266 vehicle group over time; but there were no differences observed between the Zol alone and the combination groups (Figure 5 ix). Surprisingly, there were no visible osteoblasts on either of these surfaces in any of the groups, despite the obvious repair in cortical bone lesions. Similarly, there were also no differences in the serum P1NP levels between the groups (Figure 5 x), suggesting the level of bone formation required to repair the lytic lesions was not high enough to increase systemic P1NP levels.

Overall, these data strongly demonstrate that combination therapy using TGFβ inhibition with Zol can repair existing osteolytic lesions in murine models of myeloma, a novel finding not yet reported in myeloma or other cancer-induced bone diseases.

TGFβ inhibition in combination with Zol does not alter JJN3 or U266 tumor burden in vivo

Since others have reported that TGFβ inhibition has an anti-tumor effect in vivo in models of breast cancer and myeloma (39-41), we wanted to discount that any effect we observed was due to a reduction in tumor burden. Therefore, we quantified localized tumor burden in the JJN3 and U266 models by flow cytometry (Figure 6a i-ix) and histological morphology (Figure 6b i-vi). In addition, in the U266 model we quantified systemic human IgE paraprotein by ELISA (Figure 6b vii). By all methods and in both models assessed, Zol or 1D11 monotherapies or in combination had no significant effect upon tumor burden. Therefore, this indicates that all bone effects observed in our studies were a direct effect upon bone itself and not as a result of reduced tumor burden. To confirm this, we also treated JJN3 and U266 cells in vitro with vehicle, IC or 1D11 and no significant effects on cell viability for either cell line were observed (Figure 6 viii, ix).

Discussion

Multiple myeloma remains a largely incurable bone marrow cancer, which causes devastating bone disease resulting in a substantially diminished quality of life for most patients. The current standard of care for bone disease is antiresorptive therapy, usually the bisphosphonate Zol. However, antiresorptive therapy alone does not repair existing bone damage, meaning bones remain weak and are prone to fracture. Previously, bone anabolic therapy using parathyroid hormone (PTH) or anti-sclerostin (Romosuzumab) showed improved bone outcomes in patients with metabolic disorders such as osteoporosis (20, 61-63). In addition, anti-sclerostin therapy in preclinical models of myeloma using preventative treatment strategies have inhibited bone loss and increased bone strength (25, 63), highlighting that bone anabolic therapy could be of great benefit to patients with myeloma bone disease.

In the studies presented here, we have shown for the first time that the bone anabolic 1D11 (anti-TGFβ antibody), when administered in combination with the antiresorptive Zol, provided a therapeutic strategy for both the prevention, but more importantly, in the treatment of myeloma-induced bone disease. We firstly verified that rTGFβ inhibited osteoblast differentiation as shown previously (39, 58, 64) and that this could be prevented using 1D11, which correlated with previous in vitro osteoblast assays using TGFβ small molecule inhibitors (39). In addition, we showed that 1D11 alone increased BV/TV in naïve NSG mice, supporting data by Edwards et al. (29) who looked at the effect in C57BL/6 naïve mice; and 1D11 monotherapy also prevented bone loss in the JJN3 model of myeloma, which corresponded with previous studies using the 5TGM1 model of myeloma (46). Most importantly, we found that when 1D11 was administered in combination with Zol, this therapeutic strategy significantly enhanced BV/TV in the JJN3 model of myeloma; and treated bone disease and repaired osteolytic lesions in the U266 model of myeloma, a finding not yet reported in the literature. In addition, this effect was not mediated by a reduction in tumor burden, which did not alter following 1D11/combination treatment groups, consistent with other findings in myeloma (46). However, this lack of effect upon tumor burden is somewhat contradictory to some other studies in myeloma (38, 39) and breast cancer models (65, 66), which did observe an anti-tumor effect. To confirm whether 1D11 had a direct anti-tumor effect on JJN3 or U266 cells we treated them with 1D11 in vitro, and observed no effect on cell viability for either cell line. Therefore, 1D11 does not directly influence tumor growth in vitro or in vivo and these discrepancies with previous studies in anti-tumor effects may be due differential regulation of factors implicated in tumor cell proliferation including PTHrP (41), IL-6 (37) or Notch (67), that are controlled by TGFβ signalling, which may vary between tumor cell types and mice strains. In addition, others have observed that the anti-tumor effects of 1D11 may be dependent on the tumor location (68), the presence of other cells (68-70), disruption of key signalling

pathways (71) and when 1D11 treatment commences (69). Therefore, there are potentially a number of reasons why we did not observe an anti-tumor effect in our in vivo studies.

A potential limitation of our studies is they were all performed in immunocompromised mice. However, the rational for using these models was based on the marked destructive osteolytic bone lesions that both JJN3 and U266 models feature (51) compared to the immune competent 5TGM1 model which has a less pronounced bone disease (72). In addition, to monitor lesion repair a larger therapeutic window was required from onset of established osteolytic lesions to the end stage of disease. In the 5TGM1 model this is only a few days (17-21 days post 5TGM1 cell injection) (72), whereas in the U266 model used here it was for approximately 3 weeks (6-9 weeks post U266 cell injection). Therefore, this provided us with a larger treatment window in order to clearly determine the effects of combined 1D11 and Zol treatment on bone repair. In addition, Zol and 1D11 (as well as SD-208, a small inhibitor to TGFβ receptor type 1) have previously been used in immune competent mice. For example, Edwards et al., have assessed 1D11 in naïve mice and Nyman et al.,(46) have assessed 1D11 in the 5TGM1 model. Similarly, we have previously assessed the effects of Zol in immunocompromised mice (51, 73) and shown similar effects on bone to immune competent mice (74). Therefore, we would expect to observe similar effects on bone in immune competent animals treated with combined 1D11 and Zol.

Our studies clearly demonstrate the benefits of combined 1D11 and Zol treatment on bone, yet the exact mechanism by which the repair of bone occurs remains unclear. Monotherapy of Zol or 1D11 in the JJN3 model of MM resulted in a reduction in osteoclasts, consistent with previous findings by Mohammed et al. (75) and Edwards et al. (29) using SD-208/1D11 in naïve mice. In the 1D11 monotherapy group, this was potentially mediated by a reduction in

IL-6 levels, a finding described previously when SD-208 blocked TGFβ1 induced secretion of IL-6 by BMSC in vitro (39). Nevertheless, in our in vivo studies we were unable to identify an increase in osteoblast numbers or P1NP sera levels (markers of bone formation) in these studies, despite clear enhancement of bone formation. We suspect that this may be because our sacrifice time points did not coincide with the precise time points at which osteoblast numbers, or biomarker levels, were increased, as well as lack of sensitivity in the sera analysis. In addition, when early and late osteocyte patterns were examined by anti-sclerostin and anti-E11 immunohistochemical staining no differences were found following 1D11 treatment (data not shown), and sclerostin sera levels were also unchanged between the groups (data not shown), highlighting that there were no significant changes in osteocytes following 1D11 treatment. Studies by Nyman et al. (46) did observe an increase in osteoblasts following TGFβ inhibition, but their studies differed to ours in mouse strain (C57BL/KalwRij), cell line (5TGM1) and inhibitor (SD-208), which could have affected the osteoblast analysis. Therefore, we strongly believe that the additive effect observed in both myeloma models is due to both an inhibitory effect on osteoclasts and a substantial anabolic effect on osteoblastic bone formation. The latter is likely to have occurred early after treatment and thus has not been captured at the end stage of disease when tumor burden is high.

Nevertheless, the overall findings described here show a highly translational approach for the use of bone anabolic and antiresorptive therapy to prevent and repair myeloma-induced bone disease, particularly as anti-TGFβ therapy using a humanised antibody (GC1008) is currently in clinical trials in breast cancer (NCT01401062) (44, 45). Furthermore, we are now exploring the optimum sequencing approach of bone anabolic and antiresorptive therapies, given promising data emerging from clinical trials in patients with osteoporosis (76, 77). We strongly believe that combination therapy delivered in the optimum sequence has the potential

to substantially improve patient prognosis by reducing fracture risk, reducing pain, increasing

functional status and thus providing a very considerable overall improvement in quality of life

for those with this devastating aspect of myeloma.

Authors' roles

ML, AC, JS conceived the project. JPH and ST designed and performed experiments and analyzed and interpreted the data. JPH wrote manuscript. HE and AG were responsible for μCT analysis. JD and DL conducted histological analysis. ML, AC, JS, JPH, ST, HE, AG, JD and DL revised and approved the final manuscript.

References

1.   Mercadante S. Malignant bone pain: pathophysiology and treatment. Pain. 1997;69(1):1-18.

2.   Roodman GD. Pathogenesis of myeloma bone disease. Leukemia. 2009;23(3):435-41.

3.   Melton LJ, Kyle RA, Achenbach SJ, Oberg AL, Rajkumar SV. Fracture Risk With Multiple Myeloma: A Population-Based Study. Journal of Bone and Mineral Research. 2005;20(3):487-93.

4.   Saad F, Lipton A, Cook R, Chen YM, Smith M, Coleman R. Pathologic fractures correlate with reduced survival in patients with malignant bone disease. Cancer. 2007;110(8):1860-7.

5.   Sezer O, Heider U, Jakob C, Zavrski I, Eucker J, Possinger K, et al. Immunocytochemistry reveals RANKL expression of myeloma cells. Blood. 2002;99(12):4646-7.

6.   Croucher P, Shipman C, Lippitt J, Perry M, Asosingh K, Hijzen A, et al. Osteoprotegerin inhibits the development of osteolytic bone disease in multiple myeloma. Blood. 2001;98(13):3534.

7.   Han J, Choi S, Kurihara N, Koide M, Oba Y, Roodman G. Macrophage inflammatory protein-1 {alpha} is an osteoclastogenic factor in myeloma that is independent of receptor activator of nuclear factor {kappa} B ligand. Blood. 2001;97(11):3349.

8.   Oyajobi BO, Franchin G, Williams PJ, Pulkrabek D, Gupta A, Munoz S, et al. Dual effects of macrophage inflammatory protein-1α on osteolysis and tumor burden in the murine 5TGM1 model of myeloma bone disease. Blood. 2003;102(1):311-9.

9.   Yamamoto I, Kawano M, Sone T, Iwato K, Tanaka H, Ishikawa H, et al. Production of interleukin 1β, a potent bone resorbing cytokine, by cultured human myeloma cells. Cancer research. 1989;49(15):4242-6.

10.   Lee JW, Chung HY, Ehrlich LA, Jelinek DF, Callander NS, Roodman GD, et al. IL-3 expression by myeloma cells increases both osteoclast formation and growth of myeloma cells. Blood. 2004;103(6):2308-15.

11.   Sati HI, Apperley JF, Greaves M, Lawry J, Gooding R, Russell RGG, et al. Interleukin-6 is expressed by plasma cells from patients with multiple myeloma and monoclonal gammopathy of undetermined significance. British journal of haematology. 1998;101(2):287-95.

12.   Qian J, Xie J, Hong S, Yang J, Zhang L, Han X, et al. Dickkopf-1 (DKK1) is a widely expressed and potent tumor-associated antigen in multiple myeloma. Blood. 2007;110(5):1587-94.

13.   Tian E, Zhan F, Walker R, Rasmussen E, Ma Y, Barlogie B, et al. The role of the Wnt-signaling antagonist DKK1 in the development of osteolytic lesions in multiple myeloma. N Engl J Med. 2003;349(26):2483-94.

14.   Terpos E, Kastritis E, Christoulas D, Gkotzamanidou M, Eleutherakis-Papaiakovou E, Kanellias N, et al. Circulating activin-A is elevated in patients with advanced multiple myeloma and correlates with extensive bone involvement and inferior survival; no alterations post-lenalidomide and dexamethasone therapy. Ann Oncol. 2012;23(10):2681-6.

15.   Vallet S, Mukherjee S, Vaghela N, Hideshima T, Fulciniti M, Pozzi S, et al. Activin A promotes multiple myeloma-induced osteolysis and is a promising target for myeloma bone disease. Proceedings of the National Academy of Sciences of the United States of America. 2010;107(11):5124-9.

16.   Terpos E, Christoulas D, Katodritou E, Bratengeier C, Gkotzamanidou M, Michalis E, et al. Elevated circulating sclerostin correlates with advanced disease features and abnormal bone remodeling in symptomatic myeloma: reduction post-bortezomib monotherapy. Int J Cancer. 2012;131(6):1466-71.

17. Eda H, Santo L, Wein MN, Hu DZ, Cirstea DD, Nemani N, et al. Regulation of Sclerostin Expression in Multiple Myeloma by Dkk-1: A Potential Therapeutic Strategy for Myeloma Bone Disease. Journal of Bone and Mineral Research. 2016.

18. Morgan GJ, Davies FE, Gregory WM, Cocks K, Bell SE, Szubert AJ, et al. First-line treatment with zoledronic acid as compared with clodronic acid in multiple myeloma (MRC Myeloma IX): a randomised controlled trial. The Lancet. 2010;376(9757):1989-99.

19. Heath DJ, Chantry AD, Buckle CH, Coulton L, Shaughnessy JD, Evans HR, et al. Inhibiting Dickkopf-1 (Dkk1) removes suppression of bone formation and prevents the development of osteolytic bone disease in multiple myeloma. Journal of Bone and Mineral Research. 2009;24(3):425-36.

20. Yaccoby S, Ling W, Zhan F, Walker R, Barlogie B, Shaughnessy JD. Antibody-based inhibition of DKK1 suppresses tumor-induced bone resorption and multiple myeloma growth in vivo. Blood. 2007;109(5):2106-11.

21. Abdulkadyrov KM, Salogub GN, Khuazheva NK, Sherman ML, Laadem A, Barger R, et al. Sotatercept in patients with osteolytic lesions of multiple myeloma. Br J Haematol. 2014;165(6):814-23.

22. Iyer SP, Beck JT, Stewart AK, Shah J, Kelly KR, Isaacs R, et al. A Phase IB multicentre dose-determination study of BHQ880 in combination with anti-myeloma therapy and zoledronic acid in patients with relapsed or refractory multiple myeloma and prior skeletal-related events. Br J Haematol. 2014;167(3):366-75.

23. Sezer O, Beksac M, Hajek R, Sucak G, Cagirgan S, Linkesch W, et al. Effects of single-agent bortezomib as post-transplant consolidation therapy on multiple myeloma-related bone disease: a randomized phase II study. Br J Haematol. 2017;178(1):61-71.

24.   Delgado-Calle J, Anderson J, Cregor MD, Condon KW, Kuhstoss SA, Plotkin LI, et al. Genetic deletion of Sost or pharmacological inhibition of sclerostin prevent multiple myeloma-induced bone disease without affecting tumor growth. Leukemia. 2017.

25.   McDonald MM, Reagan MR, Youlten SE, Mohanty ST, Seckinger A, Terry RL, et al. Inhibiting the osteocyte-specific protein sclerostin increases bone mass and fracture resistance in multiple myeloma. Blood. 2017;129(26):3452-64.

26.   Ishibashi H, Crittenden DB, Miyauchi A, Libanati C, Maddox J, Fan M, et al. Romosozumab increases bone mineral density in postmenopausal Japanese women with osteoporosis: A phase 2 study. Bone. 2017;103:209-15.

27.   Saag KG, Petersen J, Brandi ML, Karaplis AC, Lorentzon M, Thomas T, et al. Romosozumab or alendronate for fracture prevention in women with osteoporosis. New England Journal of Medicine. 2017;377(15):1417-27.

28.   Florio M, Gunasekaran K, Stolina M, Li X, Liu L, Tipton B, et al. A bispecific antibody targeting sclerostin and DKK-1 promotes bone mass accrual and fracture repair. Nature communications. 2016;7.

29.   Edwards JR, Nyman JS, Lwin ST, Moore MM, Esparza J, O'Quinn EC, et al. Inhibition of TGF-beta signaling by 1D11 antibody treatment increases bone mass and quality in vivo. J Bone Miner Res. 2010;25(11):2419-26.

30.   Maeda S, Hayashi M, Komiya S, Imamura T, Miyazono K. Endogenous TGF-beta signaling suppresses maturation of osteoblastic mesenchymal cells. EMBO J. 2004;23(3):552-63.

31.   Kassem M, Kveiborg M, Eriksen E. Production and action of transforming growth factor-b in human osteoblast cultures: dependence on cell differentiation and modulation by calcitriol. European journal of clinical investigation. 2000;30(5):429-37.

32. Hock J, Canalis E, Centrella M. Transforming growth factor-beta stimulates bone matrix apposition and bone cell replication in cultured fetal rat calvariae. Endocrinology. 1990;126(1):421-6.

33. Cook G, Campbell J, Carr CE, Boyd KS, Franklin IM. Transforming growth factor beta from multiple myeloma cells inhibits proliferation and IL-2 responsiveness in T lymphocytes. Journal of leukocyte biology. 1999;66(6):981-8.

34. Urashima M, Ogata A, Chauhan D, Hatziyanni M, Vidriales M, Dedera D, et al. Transforming growth factor-beta1: differential effects on multiple myeloma versus normal B cells. Blood. 1996;87(5):1928-38.

35. Anagnostopoulos A, Evangelopoulou A, Sotou D, Gika D, Mitsibounas D, Dimopoulos M-A. Incidence and evolution of monoclonal gammopathy of undetermined significance (MGUS) in Greece. Annals of hematology. 2002;81(7):357-61.

36. Kyrtsonis M-C, Repa C, Mouzaki A, Simeonidis A, Stamatelou M, Maniatis A. Serum transforming growth factor-β1 is related to the degree of immunoparesis in patients with multiple myeloma. Medical Oncology. 1998;15(2):124-8.

37. Hayashi T, Hideshima T, Nguyen AN, Munoz O, Podar K, Hamasaki M, et al. Transforming Growth Factor β Receptor I Kinase Inhibitor Down-Regulates Cytokine Secretion and Multiple Myeloma Cell Growth in the Bone Marrow Microenvironment. American Association for Cancer Research. 2004;10(22):7540-6.

38. Lu A, Pallero MA, Lei W, Hong H, Yang Y, Suto MJ, et al. Inhibition of Transforming Growth Factor-β Activation Diminishes Tumor Progression and Osteolytic Bone Disease in Mouse Models of Multiple Myeloma. The American Journal of Pathology. 2016;186(3):678-90.

39. Takeuchi K, Abe M, Hiasa M, Oda A, Amou H, Kido S, et al. TGF-β Inhibition Restores Terminal Osteoblast Differentiation to Suppress Myeloma Growth. PLoS ONE. 2010;5(3):e9870.

40. Biswas S, Nyman JS, Alvarez J, Chakrabarti A, Ayres A, Sterling J, et al. Anti-transforming growth factor ss antibody treatment rescues bone loss and prevents breast cancer metastasis to bone. PloS one. 2011;6(11):e27090.

41. Yin JJ, Selander K, Chirgwin JM, Dallas M, Grubbs BG, Wieser R, et al. TGF-β signaling blockade inhibits PTHrP secretion by breast cancer cells and bone metastases development. Journal of Clinical Investigation. 1999;103(2):197.

42. Ganapathy V, Ge R, Grazioli A, Xie W, Banach-Petrosky W, Kang Y, et al. Targeting the transforming growth factor-β pathway inhibits human basal-like breast cancer metastasis. Molecular cancer. 2010;9(1):122.

43. Fournier PG, Juárez P, Jiang G, Clines GA, Niewolna M, Kim HS, et al. The TGF-β signaling regulator PMEPA1 suppresses prostate cancer metastases to bone. Cancer Cell. 2015;27(6):809-21.

44. Rodon J, Carducci MA, Sepulveda-Sánchez JM, Azaro A, Calvo E, Seoane J, et al. First-in-human dose study of the novel transforming growth factor-β receptor I kinase inhibitor LY2157299 monohydrate in patients with advanced cancer and glioma. Clinical Cancer Research. 2015;21(3):553-60.

45. Morris JC, Tan AR, Olencki TE, Shapiro GI, Dezube BJ, Reiss M, et al. Phase I study of GC1008 (fresolimumab): a human anti-transforming growth factor-beta (TGFβ) monoclonal antibody in patients with advanced malignant melanoma or renal cell carcinoma. PloS one. 2014;9(3):e90353.

46. Nyman JS, Merkel AR, Uppuganti S, Nayak B, Rowland B, Makowski AJ, et al. Combined treatment with a transforming growth factor beta inhibitor (1D11) and bortezomib

improves bone architecture in a mouse model of myeloma-induced bone disease. Bone. 2016;91:81-91.

47.   Yang D, Atkins G, Turner A, Anderson P, Morris H. Differential effects of 1, 25-dihydroxyvitamin D on mineralisation and differentiation in two different types of osteoblast-like cultures. The Journal of steroid biochemistry and molecular biology. 2013;136:166-70.

48.   Gartland A, Buckley KA, Dillon JP, Curran JM, Hunt JA, Gallagher JA. Isolation and culture of human osteoblasts. Human Cell Culture Protocols. 2005:29-54.

49.   Ahmad M, McCarthy M, Gronowicz G. An in vitro model for mineralization of human osteoblast-like cells on implant materials. Biomaterials. 1999;20(3):211-20.

50.   Wang N, Agrawal A, Jorgensen NR, Gartland A. P2X7 receptor regulates osteoclast function and bone loss in a mouse model of osteoporosis. Sci Rep-Uk. 2018;8.

51.   Lawson MA, Paton-Hough JM, Evans HR, Walker RE, Harris W, Ratnabalan D, et al. NOD/SCID-GAMMA mice are an ideal strain to assess the efficacy of therapeutic agents used in the treatment of myeloma bone disease. PloS one. 2015;10(3):e0119546.

52.   Paton-Hough J, Chantry A, Lawson M. A review of current murine models of multiple myeloma used to assess the efficacy of therapeutic agents on tumour growth and bone disease. Bone. 2015;77:57-68.

53.   Miyakawa Y, Ohnishi Y, Tomisawa M, Monnai M, Kohmura K, Ueyama Y, et al. Establishment of a new model of human multiple myeloma using NOD/SCID/γ c null (NOG) mice. Biochemical and biophysical research communications. 2004;313(2):258-62.

54.   Schueler J, Wider D, Klingner K, Siegers GM, May AM, Wasch R, et al. Intratibial injection of human multiple myeloma cells in NOD/SCID IL-2Rgamma(null) mice mimics human myeloma and serves as a valuable tool for the development of anticancer strategies. PloS one. 2013;8(11):e79939.

55. Bouxsein ML, Boyd SK, Christiansen BA, Guldberg RE, Jepsen KJ, Muller R. Guidelines for assessment of bone microstructure in rodents using micro-computed tomography. J Bone Miner Res. 2010;25(7):1468-86.

56. Dempster DW, Compston JE, Drezner MK, Glorieux FH, Kanis JA, Malluche H, et al. Standardized nomenclature, symbols, and units for bone histomorphometry: a 2012 update of the report of the ASBMR Histomorphometry Nomenclature Committee. J Bone Miner Res. 2013;28(1):2-17.

57. Tang Y, Wu X, Lei W, Pang L, Wan C, Shi Z, et al. TGF-β1–induced migration of bone mesenchymal stem cells couples bone resorption with formation. Nature medicine. 2009;15(7):757-65.

58. Maeda S, Hayashi M, Komiya S, Imamura T, Miyazono K. Endogenous TGF-β signaling suppresses maturation of osteoblastic mesenchymal cells. The EMBO Journal. 2004;23(3):552-63.

59. Bonewald L, Mundy G. Role of transforming growth factor-beta in bone remodeling. Clinical orthopaedics and related research. 1990;250:261-76.

60. Sezer O, Aydin AA, Bilge S, Arslan F, Arslan H. Acute dystonic reaction leading to lingual hematoma mimicking angioedema. Indian journal of pharmacology. 2017;49(4):325-7.

61. Neer RM, Arnaud CD, Zanchetta JR, Prince R, Gaich GA, Reginster J-Y, et al. Effect of parathyroid hormone (1-34) on fractures and bone mineral density in postmenopausal women with osteoporosis. New England journal of medicine. 2001;344(19):1434-41.

62. Black DM, Greenspan SL, Ensrud KE, Palermo L, McGowan JA, Lang TF, et al. The effects of parathyroid hormone and alendronate alone or in combination in postmenopausal osteoporosis. New England Journal of Medicine. 2003;349(13):1207-15.

63.   Iyer SP, Beck JT, Stewart AK, Shah J, Kelly KR, Isaacs R, et al. A Phase IB multicentre dose-determination study of BHQ880 in combination with anti-myeloma therapy and zoledronic acid in patients with relapsed or refractory multiple myeloma and prior skeletal-related events. British journal of haematology. 2014;167(3):366-75.

64.   Breen EC, Ignotz RA, McCabe L, Stein JL, Stein GS, Lian JB. TGFβ alters growth and differentiation related gene expression in proliferating osteoblasts in vitro, preventing development of the mature bone phenotype. Journal of Cellular Physiology. 1994;160(2):323-35.

65.   Biswas S, Nyman JS, Alvarez J, Chakrabarti A, Ayres A, Sterling J, et al. Anti-Transforming Growth Factor ß Antibody Treatment Rescues Bone Loss and Prevents Breast Cancer Metastasis to Bone. PLoS ONE. 2011;6(11):e27090.

66.   Yin JJ, Selander K, Chirgwin JM, Dallas M, Grubbs BG, Wieser R, et al. TGF-β signaling blockade inhibits PTHrP secretion by breast cancer cells and bone metastases development. The Journal of Clinical Investigation.103(2):197-206.

67.   Sethi N, Dai X, Winter CG, Kang Y. Tumor-derived jagged1 promotes osteolytic bone metastasis of breast cancer by engaging notch signaling in bone cells. Cancer cell. 2011;19(2):192-205.

68.   Hulper P, Schulz-Schaeffer W, Dullin C, Hoffmann P, Harper J, Kurtzberg L, et al. Tumor localization of an anti-TGF-beta antibody and its effects on gliomas. Int J Oncol. 2011;38(1):51-9.

69.   Buenrostro D, Kwakwa KA, Putnam NE, Merkel AR, Johnson JR, Cassat JE, et al. Early TGF-beta inhibition in mice reduces the incidence of breast cancer induced bone disease in a myeloid dependent manner. Bone. 2018;113:77-88.

70. Chen X, Yang Y, Zhou Q, Weiss JM, Howard OZ, McPherson JM, et al. Effective chemoimmunotherapy with anti-TGFbeta antibody and cyclophosphamide in a mouse model of breast cancer. PloS one. 2014;9(1):e85398.

71. Tabe Y, Shi YX, Zeng Z, Jin L, Shikami M, Hatanaka Y, et al. TGF-beta-Neutralizing Antibody 1D11 Enhances Cytarabine-Induced Apoptosis in AML Cells in the Bone Marrow Microenvironment. PloS one. 2013;8(6):e62785.

72. Paton-Hough J, Chantry AD, Lawson MA. A review of current murine models of multiple myeloma used to assess the efficacy of therapeutic agents on tumour growth and bone disease. Bone. 2015.

73. Lawson MA, Ebetino FH, Mazur A, Chantry AD, Paton-Hough J, Evans HR, et al. The Pharmacological Profile of a Novel Highly Potent Bisphosphonate, OX14 (1-Fluoro-2-(Imidazo-[1,2-alpha]Pyridin-3-yl)-Ethyl-Bisphosphonate). J Bone Miner Res. 2017.

74. Croucher PI, De Hendrik R, Perry MJ, Hijzen A, Shipman CM, Lippitt J, et al. Zoledronic acid treatment of 5T2MM-bearing mice inhibits the development of myeloma bone disease: evidence for decreased osteolysis, tumor burden and angiogenesis, and increased survival. J Bone Miner Res. 2003;18(3):482-92.

75. Mohammad KS, Chen CG, Balooch G, Stebbins E, McKenna CR, Davis H, et al. Pharmacologic Inhibition of the TGF-β Type I Receptor Kinase Has Anabolic and Anti-Catabolic Effects on Bone. PLoS ONE. 2009;4(4):e5275.

76. Cosman F, Crittenden DB, Adachi JD, Binkley N, Czerwinski E, Ferrari S, et al. Romosozumab Treatment in Postmenopausal Women with Osteoporosis. N Engl J Med. 2016;375(16):1532-43.

77. Cosman F, Nieves JW, Dempster DW. Treatment Sequence Matters: Anabolic and Antiresorptive Therapy for Osteoporosis. J Bone Miner Res. 2017;32(2):198-202.

Conflicts of Interest

There are no conflicts of interest by any author.

Figure legends

Figure 1. Administration of anti-TGFβ (1D11) prevented rTGFβ inhibition of osteoblastic alkaline phosphatase production and mineralisation in vitro, and resulted in a substantial bone anabolic effect in vivo. (**a**) Alp production in primary murine Ob-LC cultured in osteogenic media with vehicle (CTRL), rTGFβ and IC antibody (rTGFβ + IC) or rTGFβ and 1D11 antibody (rTGFβ + 1D11) for 7 (**i**) and 14 days (**ii**). Alp production in SAOS-2 cells cultured in standard media and treated as above for 3 days (**iii**). Mineralisation in Ob-LC treated as above for 14 (**iv**) and 21 days (**v**). Representative images of mineralisation in Ob-LC treated as above (**vi**). All data is representative from four independent experiments, presented as mean fold change ± SD, one-way ANOVA, **p≤ 0.01, ***p≤ 0.001 and ****p≤ 0.0001. (**b**) Schematic demonstrating the treatment schedule for 1D11 monotherapy treatment in Naïve mice and the JJN3 model of myeloma. (**c**) Representative 3-D trabecular μCT images from the tibiae of Naïve+IC (**i**), Naïve+1D11 (**ii**), JJN3+IC (**iii**) and JJN3+1D11 (**iv**) mice. BV/TV (**v**), trabecular number (**vi**) and trabecular thickness (**vii**) analyzed in the tibiae by μCT. All data are presented as mean ± SD, Student's T-test, **p≤ 0.001 and ***p≤ 0.001.

Figure 2. Administration of anti-TGFβ (1D11) in combination with Zol significantly increased BV/TV compared to monotherapy in the JJN3 model of myeloma. (**a**) Schematic demonstrating the treatment schedule for Zol or 1D11 monotherapies or in combination in the JJN3 model of myeloma. (**b**) Representative 3-D trabecular bone μCT images from the tibiae of JJN3+vehicle (JJN3) (**i**), JJN3+Zol (Zol) (**ii**), JJN3+1D11 (1D11) (**iii**) and JJN3+1D11+Zol (Combo) (**iv**) mice. BV/TV (**v**), trabecular number (**vi**) and trabecular thickness (**vii**) analyzed in the tibiae by μCT. (**c**) Representative 3-D transverse cortical and trabecular bone μCT images from the tibiae of JJN3 (**i**), Zol (**ii**), 1D11 (**iii**) and Combo (**iv**) mice, blue arrows show

areas of bone loss and green arrows show areas of new bone formation. Cortical thickness (**v**), lesion number (**vi**) and lesion area (**vii**) analyzed in the tibiae by μCT. All data are presented as mean ± SD, one-way ANOVA and Tukey's multiple comparison test, *p≤ 0.05, **p≤ 0.01, ***p≤ 0.001 and ****p≤ 0.0001.

Figure 3. Zol and 1D11 combination therapy did not significantly increase bone formation or decrease bone resorption compared to monotherapies in the JJN3 model of myeloma. (**a**) Representative histological images of tibia sections from JJN3-bearing mice treated with IC (**i, v**), Zol (**ii, vi**), 1D11 (**iii, vii**) and Combo (**iv, viii**), at x20 magnification (**i-iv**) and x40 magnification (**v-viii**) showing tumor bone marrow (TBM) and cortical bone (CB). Number of osteoblasts on the endocortical surface (**ix**) and on the bone primary spongiosa (**x**). Number of TRAP positive osteoclasts on the endocortical surface (**xi**) and on the primary spongiosa (**xii**). (**b**) Murine TRAP5b (**i**) present in murine sera when detected by sandwich ELISA. Primary murine osteoclast numbers (**ii**) and resorption area (**iii**) after treatment with vehicle (CTRL), IC or 1D11 after 3 days. Murine P1NP (**iv**) and murine IL-6 (**v**) present in murine sera when detected by sandwich ELISA. All data are presented as mean ± SD, one-way ANOVA, *p≤ 0.05, **p≤ 0.01, ***p≤ 0.001 and ****p≤ 0.0001.

Figure 4. Zol and 1D11 combination therapy repaired osteolytic bone lesions in the U266 murine model of myeloma. (**a**) Schematic demonstrating the treatment schedule for Zol monotherapy or Zol and 1D11 combined (Combo) in the U266 model of myeloma. (**b**) **W0**: Time of bone disease presentation (approximately 6 weeks post-U266 injection). **W3**: 3 weeks following treatment. Representative 3-D transverse cortical and trabecular registered in vivo μCT images from the tibiae of U266 vehicle W0 (U266 W0) (**i**), U266 vehicle W3 (U266 W3) (**ii**), U266+Zol W0 (Zol W0) (**iii**), U266+Zol W3 (Zol W3) (**iv**), U266+Combo W0 (Combo

W0) (**v**) and U266+Combo W3 (Combo W3) (**vi**) mice. (**c**) Representative longitudinal in vivo μCT images from the tibiae of U266 W0 (**i**), U266 W3 (**ii**), Zol W0 (**iii**), Zol W3 (**iv**), Combo W0 (**v**) and Combo W3 (**vi**) mice. Blue arrows represent initial bone disease, pink arrows represent progressive bone disease and green arrows represent a reduction in bone disease and lesion repair. Percentage change in lesion area (**vii**) from W0 to W3 by in vivo μCT, following image registration. Percentage change in cortical thickness (**viii**) from W0 to W3 by in vivo μCT. Percentage change in BV/TV (**ix**) from W0 to W3 by in vivo μCT. All data are presented as mean ± SD, Kruskal-Wallis and Dunn's multiple comparison tests, *p≤ 0.05 and **p≤ 0.01.

Figure 5. Zol and 1D11 combination therapy did not significantly decrease bone resorption or increase bone formation compared to monotherapy in the U266 model of myeloma. Representative histological images of tibiae from U266-bearing mice treated with IC (U266) (**i, iv**), Zol (**ii, v**), and Combo (**iii, vi**), at x20 magnification (i-iii) and x40 magnification (**iv-vi**). (**vii**) Number of TRAP positive osteoclasts on the endocortical surface and (**viii**) on primary spongiosa. (**ix**) Murine TRACP5b and (**x**) murine P1NP present in murine sera detected by sandwich ELISA. All data are presented as mean ± SD, ANOVA and Tukey's multiple comparison, *p≤ 0.05 and ****p≤ 0.0001.

Figure 6. 1D11 did not inhibit the growth of JJN3 or U266 cells in vivo or in vitro. (a) Representative flow cytometry dots plots showing HLA positive tumor cells from femora bone marrow flushes from JJN3-bearing (**i-iv**) or U266-bearing mice (**vi-viii**) treated with IC (JJN3 or U266) (**i, vi**), Zol (**ii, vii**), 1D11 (**iii**), Combo (**iv, viii**), quantified as a percentage of tumor burden (**v, ix**). (**b**) Representative paraffin-embedded haematoxylin stained bone marrow sections taken from Naive (**i x2, iii, x40**) or JJN3/U266-bearing mice (**ii x2, iv x40**) demonstrating how percentage of tumor area is quantified using Image Scope software, normal

marrow circled in black (**i**), bone area in circled green (**i, ii**), tumor area circled in red (**ii**). Quantification of histological tumor burden in paraffin-embedded tibiae sections taken from JJN3-bearing mice (**v**) or U266-bearing mice (**vi**) and treated with IC, Zol, 1D11 or Combo, quantified using Image Scope Software, as shown above, displayed as a percentage of tumor in the bone marrow compared to normal marrow. IgE paraprotein present in the sera of U266-bearing mice at the end stage of disease, treated with IC, Zol or Combo and analyzed by ELISA (**vii**). In vitro culture of JJN3 (**viii**) and U266 (**ix**) cells treated with vehicle (CRTL), IC or 1D11 for 4 h, 24 h, 48 h and 72 h. All data are presented as mean ± SD.
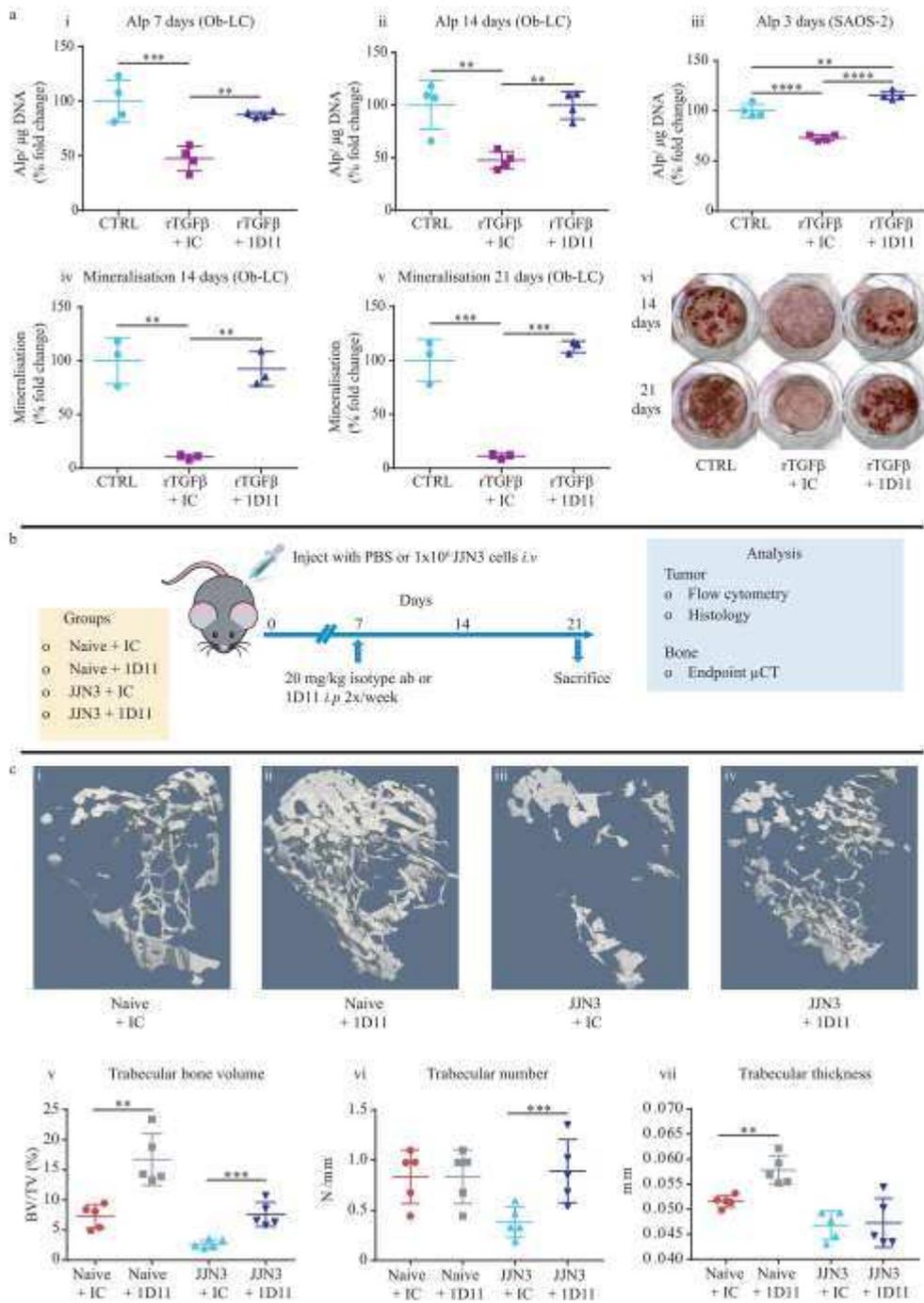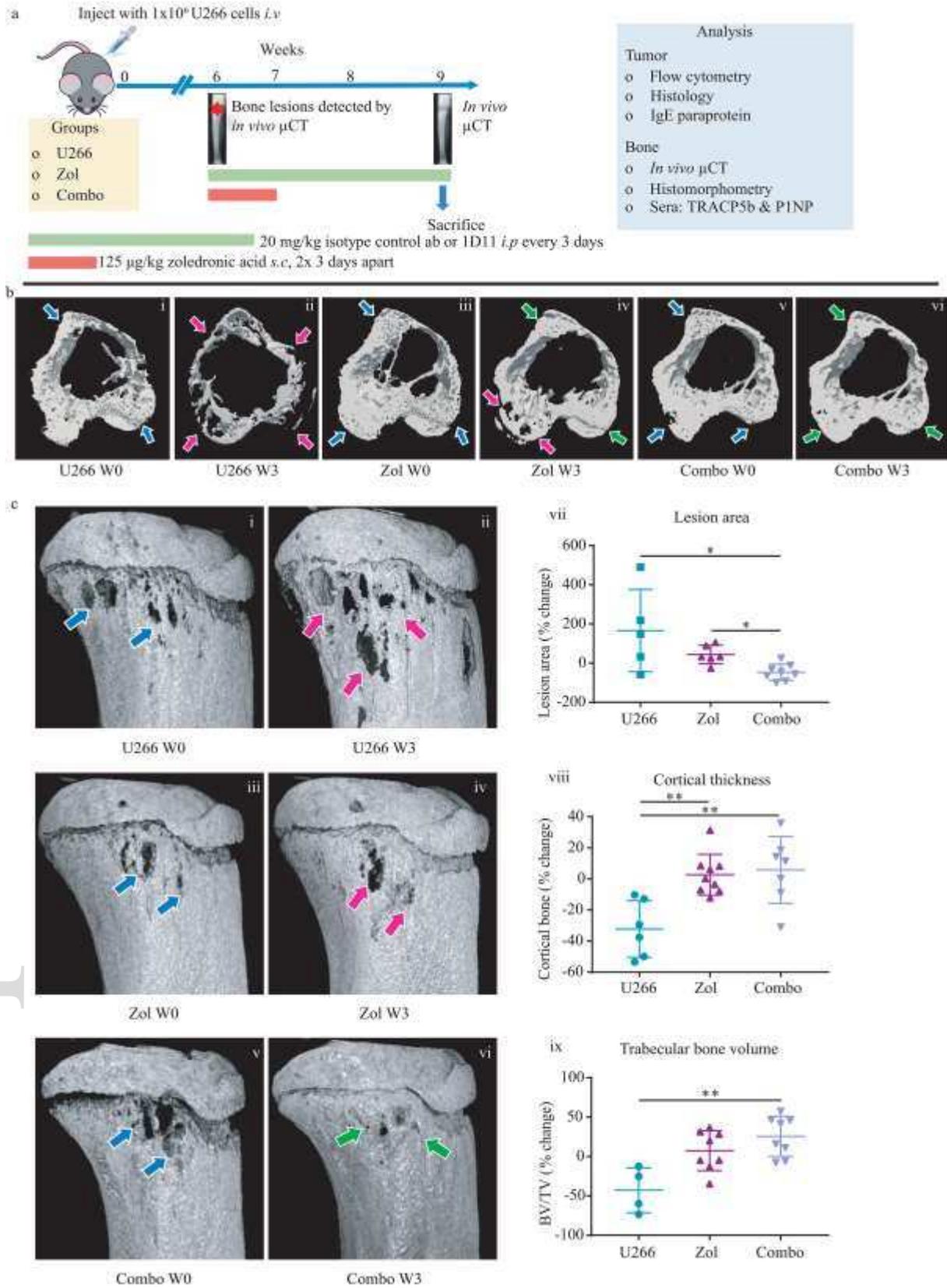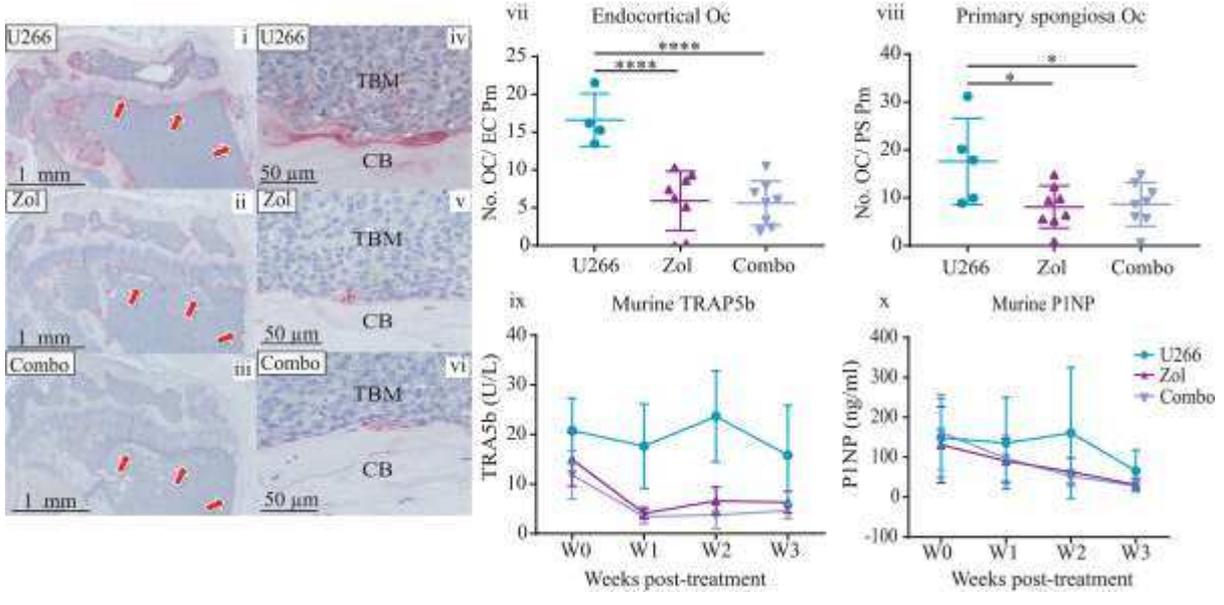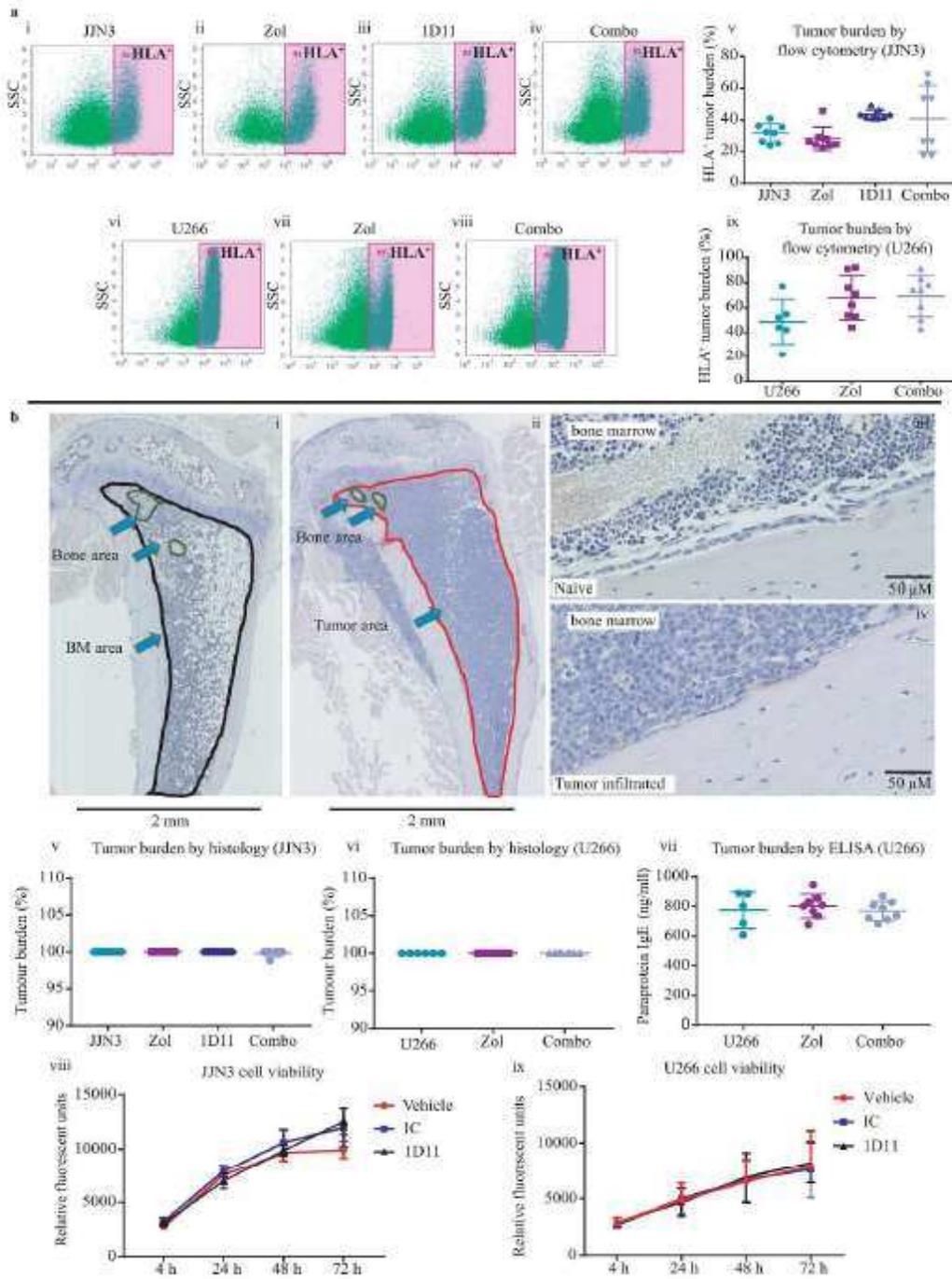
Figure 1
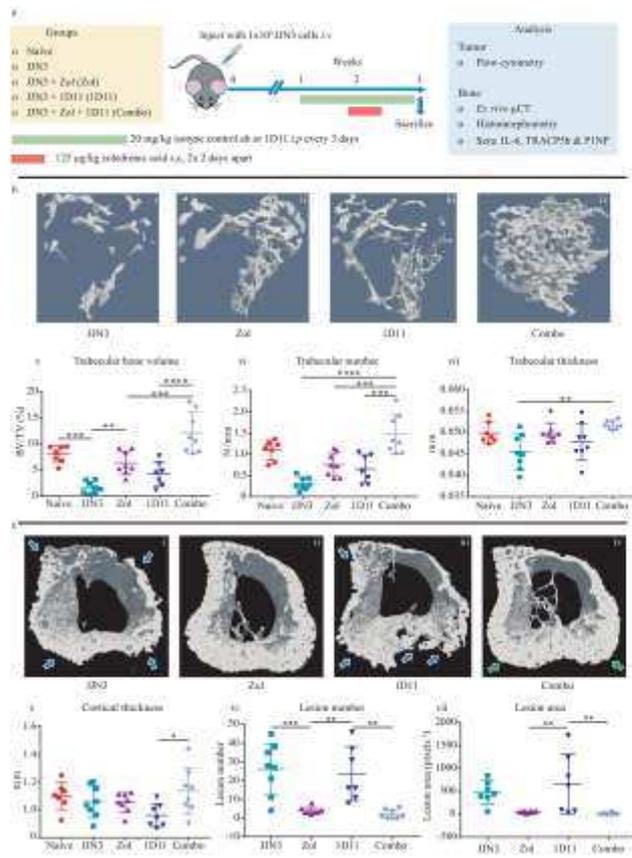
Figure 2
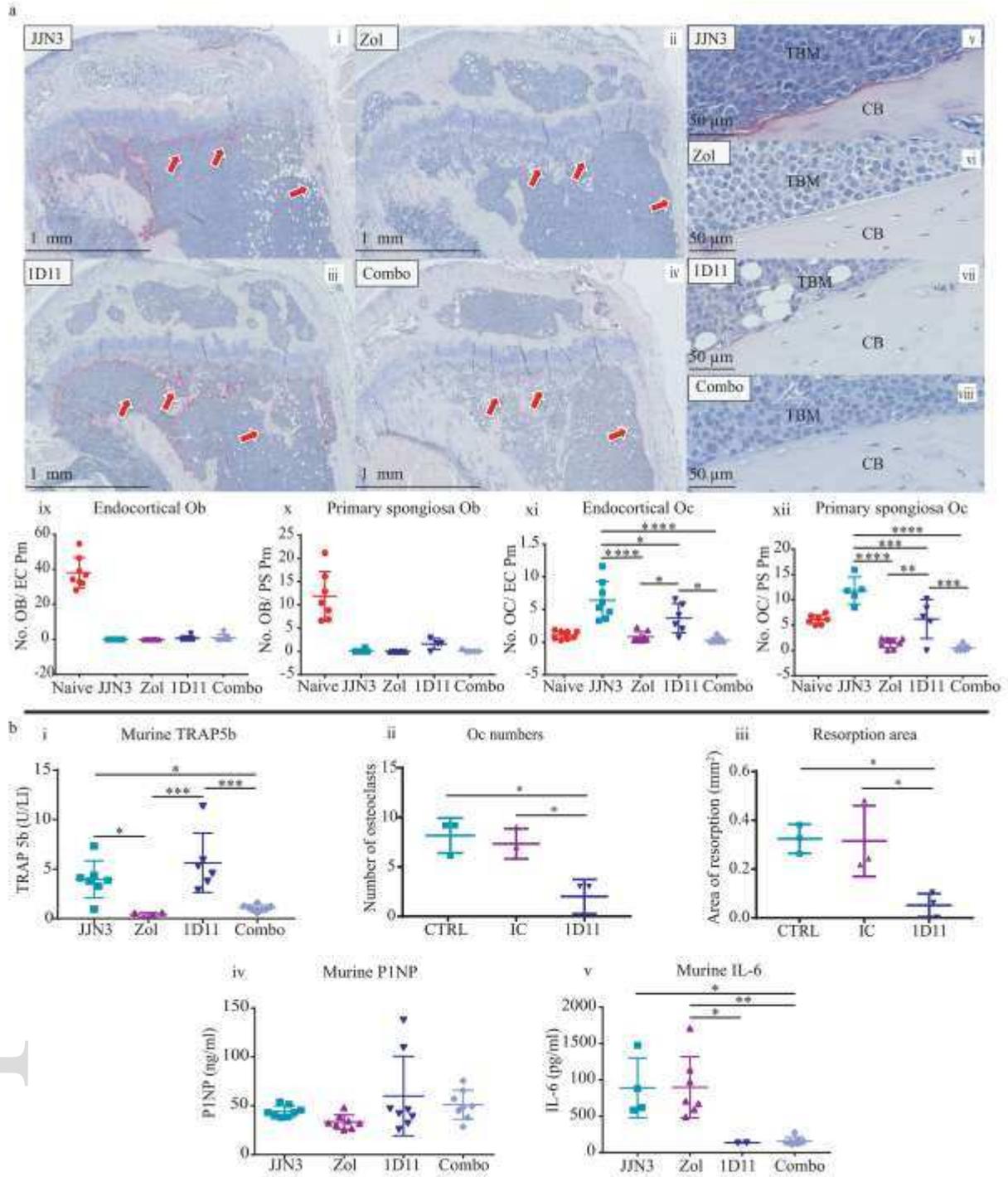
Figure 3

Figure 4

Figure 5

Figure 6